OL Organic Letters

pubs.acs.org/OrgLett Letter

Synthesis and Properties of Achiral and Chiral Dipyrenoheteroles and Related Compounds

Ryan J. Malone, Jonas Spengler, Rachael A. Carmichael, Khoa Ngo, Frank Würthner, and Wesley A. Chalifoux*

Cite This: *Org. Lett.* 2023, 25, 226–230 Read Online

ACCESS | Metrics & More | Article Recommendations | Supporting Information

ABSTRACT: Achiral and chiral isomers of dipyrenoheteroles were synthesized via alkyne benzannulation. The electronic properties of these compounds were examined using cyclic voltammetry and differential pulse voltammetry. The enantiomers of the chiral isomers were separated, and their optical properties were examined in circular dichroism and circularly polarized luminescence studies. The chiral isomers exhibited a large bathochromic shift, relative to the achiral isomer, in both absorbance and fluorescence, resulting from decreased symmetry, rather than a change in the size of the backbone.

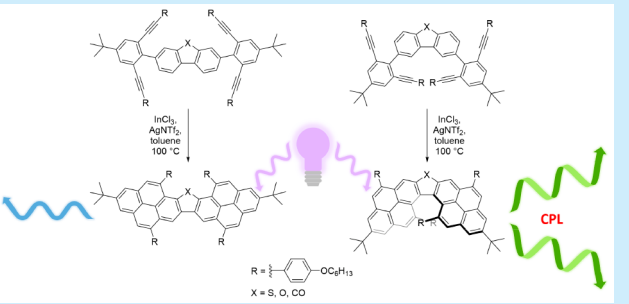

In the design of organic electronics, there is particular interest in polycyclic aromatic hydrocarbons (PAHs) based on fluorenone and dibenzoheterole precursors. Derivatives of these compounds have found their way into the design of organic field effect transistors (OFETs), organic light-emitting diodes (OLEDs), and organic photovoltaics (OPVs) through expansion of their conjugated π-electron systems.[1−3] The resulting PAHs can act as charge transport materials and allow devices that are thinner, more flexible, and more versatile than their inorganic counterparts.

Also of interest are PAHs, in which the conjugated system has been constructed in a helical fashion, leading to chirality and interesting optical properties such as circularly polarized luminescence (CPL).[4−7] Recently, CPL-active materials have attracted more interest in the design of high-efficiency OLEDs, chemical and biological sensors, and optical information processing technologies.[8,9]

In recent years, our groups have reported the synthesis of chiral perylene bisimides and structurally related chiral peropyrenes.[10−14] The latter were synthesized via 4-fold alkyne benzannulation (Figure 1a) wherein the bay regions of the peropyrene are functionalized by bulky aryl groups, creating a barrier to racemization that is sufficient for the separation of enantiomers by chiral HPLC. More recently, the Nevada team reported the use of alkyne benzannulation to laterally expand the π-electron systems of [4]helicenes while functionalizing the resulting cove regions (Figure 1b,c).[15,16] This functionalization increases the barrier of enantiomerization well beyond that of normal [4]helicene, allowing for the separation and analysis of enantiomers.

Herein, we expand upon this work, incorporating both fluorenone and dibenzoheterole subunits to access novel PAHs with bent and chiral, [5]helicene-like geometries around a central, conjugated bridging group. We have synthesized two regioisomers to examine the effects of various bridging groups and substitution patterns on the reactivity of the intermediates and the interesting changes in the optical and electronic properties of the final products.

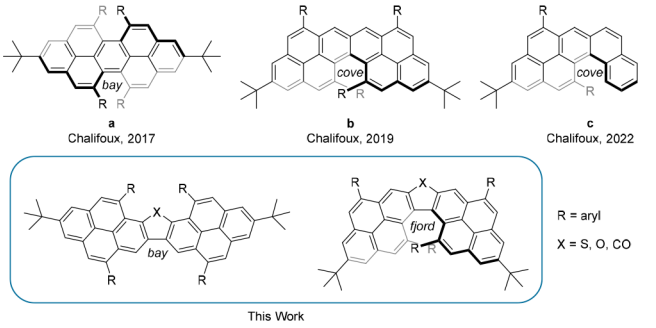

Figure 1. Twisted PAHs synthesized by the Chalifoux group. (a) Chiral peropyrene. (b) Pyreno[1,2-*a*]pyrene. (c) Naphtho[1,2-*a*]pyrene. (This Work) Dipyreno[1,2-*b*;2,1-*d*]heteroles and dipyreno-[2,1-*b*;1,2-*d*]heteroles.

Tetrayne precursors **3a−c** were obtained in good yields (72−76%) via 2-fold Suzuki cross-coupling of **2** with

Received: November 30, 2022
Published: January 3, 2023

https://doi.org/10.1021/acs.orglett.2c04071
Org. Lett. 2023, 25, 226−230

commercially available **1a–c** (Scheme 1).[17] Fourfold alkyne benzannulation was achieved by treating tetrayne precursors

Scheme 1. Synthesis of Bent-Geometry Compounds

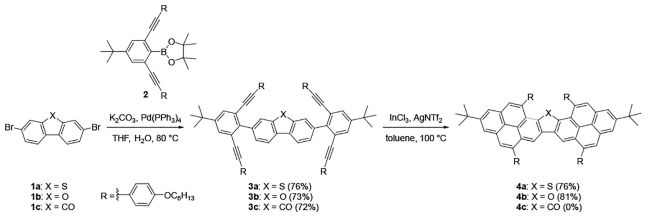

with $InCl_3$ and $AgNTf_2$, and the resulting dipyrenoheterole nanographenes **4a** and **4b** were obtained in good yields of 76% and 81%, respectively.[18,19] The calculated structures of these compounds exhibit a twist in the backbone. However, the barriers of enantiomerization are believed to be so low as to render the compounds achiral. Nanographene **4c** was not obtained due to the electronics of the core. The presence of a carbonyl *ortho* and *para* to the benzannulation reaction sites withdraws electron density from these positions, making them too unreactive for complete benzannulation to occur and resulting in a complex mixture of products.

Tetrayne precursors **6a–c** were obtained in good yields (80–85%) via 2-fold Suzuki cross-coupling of **2** with commercially available **5a–c** (Scheme 2). Fourfold alkyne

Scheme 2. Synthesis of Helicene Compounds

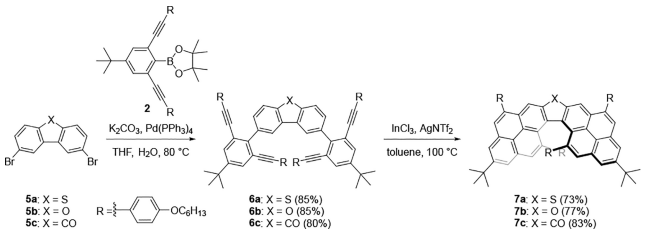

benzannulation was achieved for nanographenes **7a–c** in good yields (73–83%). Compared to those in **3c**, the reaction sites in **6c** experience a smaller electron-withdrawing effect from the carbonyl, allowing for facile benzannulation to compound **7c**, albeit with a reaction time that is longer than those of electron-rich analogues **7a** and **7b**.

In all cases of successful benzannulation, we observed a bathochromic shift in the absorbance and fluorescence spectra of **4a**, **4b**, and **7a–c**, relative to their tetrayne precursors **3a**, **3b**, and **6a–c**, respectively (Figure 2). This bathochromic shift is expected, due to the expansion of the π-electron systems. Notable, however, is the degree to which the spectra were shifted for the different regioisomers (Figure 2b,c). In 2016, the Chalifoux group showed that there is an absorbance bathochromic shift of approximately 110 nm when we expand the π-electron system of pyrene to peropyrene and again when we expand it to teropyrene.[17] In each case, we are adding three fused rings to the system. However, in the case of this work, the π-electron systems of our isomers are identical in size, yet we observed drastic changes in the absorbance and fluorescence.

When comparing **4a** and **7a**, we observed bathochromic shifts of 95 and 83 nm in the absorbance and fluorescence, respectively. Similarly, between **4b** and **7b**, we observed

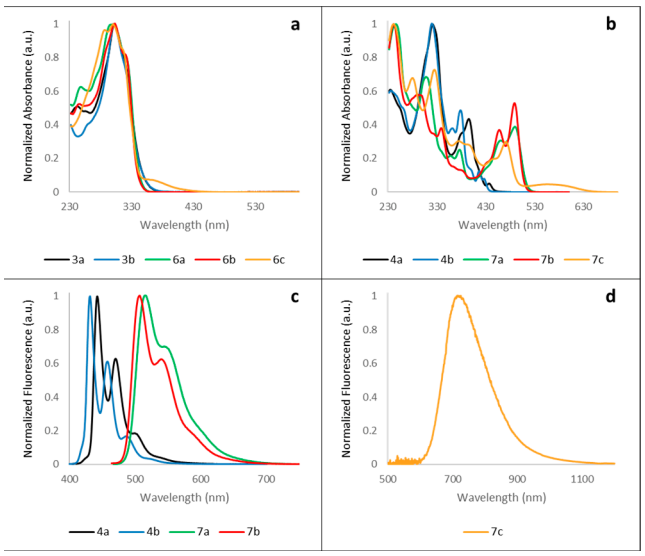

Figure 2. (a) Normalized UV–vis spectra of tetraynes measured in CH_2Cl_2 at 293 K. (b) Normalized UV–vis spectra of final compounds measured in CH_2Cl_2 at 293 K. (c) Normalized fluorescence spectra of **4a** (λ_{ex} = 396 nm), **4b** (λ_{ex} = 380 nm), **7a** (λ_{ex} = 462 nm), and **7b** (λ_{ex} = 472 nm) in a CH_2Cl_2 solution at 293 K. (d) Normalized fluorescence spectrum of **7c** (λ_{ex} = 472 nm) in a CH_2Cl_2 solution at 293 K.

bathochromic shifts of 111 and 64 nm in the absorbance and fluorescence, respectively. This phenomenon is known for isomers of relatively small PAHs wherein one isomer has a greater degree of symmetry. The less symmetrical isomer tends to be bathochromically shifted, corresponding to a smaller optical band gap.[20] The structures of compounds **4a**, **4b**, and **7a–c** were calculated at the B3LYP/6-31G(d) level of theory (Figure SI-6). The twisting of the backbone in the fjord region leads to decreased symmetry in **7** relative to the achiral isomer, **4**, so our findings are in agreement with the aforementioned trend. These results demonstrate that we can exercise a great deal of control over the optical properties of PAHs through simple changes in the geometry of the backbone, rather than changes in the size of the backbone, to give us an additional means of tuning the properties of a PAH for a given application.

The emission lifetimes and fluorescence quantum yields were determined for each benzannulated compound, and the results are listed in Table 1. In comparing **4a** and **4b** to **7a** and

Table 1. Fluorescence Lifetimes and Quantum Yields in CH_2Cl_2 Solutions at 293 K

compound	λ_{ex} (nm)	λ_{em} (nm)	τ (ns)	Φ_{Fl} (%)
4a	378.2	433	4.68	8
4b	378.2	443	8.85	20
7a	479.7	516	2.49	50
7b	479.7	507	3.54	53
7c	479.7	720	0.79	1

7b, we see that the chiral isomers exhibit fluorescence with shorter lifetimes, but with quantum yields much larger than those of their respective achiral isomers. In the case of **7c**, we observed a very short lifetime with a very low quantum yield.

The electrochemical properties of **4** and **7** were determined by cyclic voltammetry (CV) (Figure 3) and differential pulse

https://doi.org/10.1021/acs.orglett.2c04071
Org. Lett. 2023, 25, 226–230

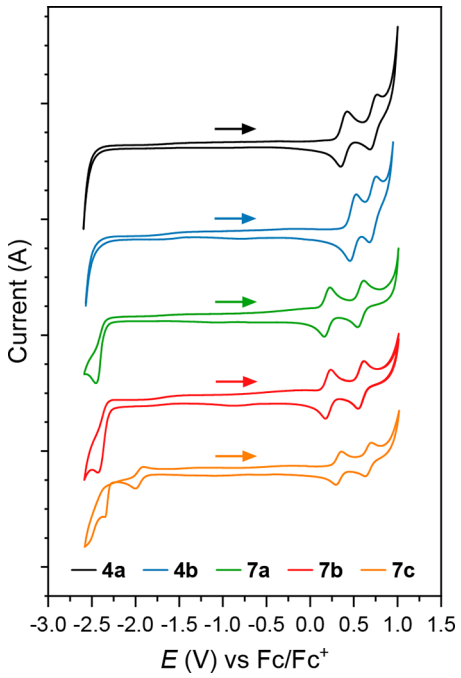

Figure 3. Cyclic voltammograms of **4a**, **4b**, and **7a**–**c** [$c \approx 2.5 \times 10^{-3}$ M, 0.1 M $(n\text{-Bu})_4NPF_6$ in CH_2Cl_2] depicted via the IUPAC convention (the direction of the scan is indicated by arrows; starting point, −2.6 V).

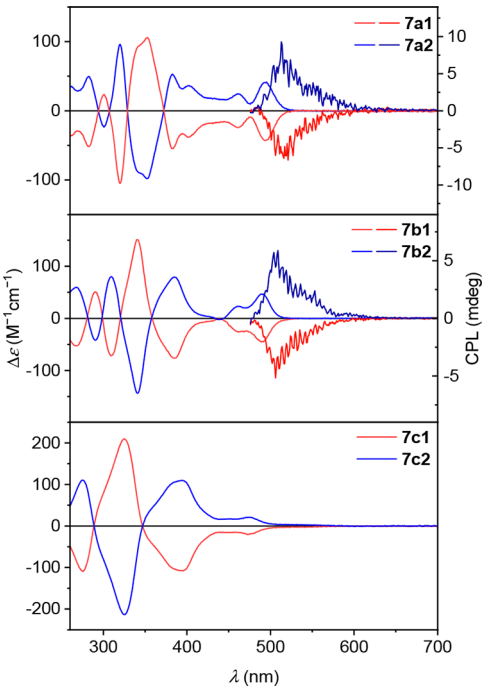

Figure 4. CD (light red and blue lines) and CPL (dark red and blue lines) of **7a**–**c** in CH_2Cl_2 at 293 K. Due to the low quantum yield of **7c** (Φ_{Fl} = 1%), no CPL data could be recorded.

voltammetry (DPV) (Figure SI-1) and are referenced versus the ferrocene/ferrocenium redox couple. The voltammograms are shown in Figure 3, and the results are summarized in Table 2. In all cases, these compounds exhibited two reversible oxidations. However, conclusive reduction peaks were observed for only **7**. Compound **7c** exhibited two reduction peaks, the first of which was reversible, whereas **7a** and **7b** showed only one irreversible reduction peak. In changing the geometry of the isomers, we observed a slight decrease in the HOMO values of **7a**–**c** relative to those of **4a** and **4b** and a decrease in the LUMO values of **7a**–**c** relative to those of **4a** and **4b** because no reduction waves were observed in the probed electrochemical window. From these results, we have further confirmation that changing the shape of the conjugated backbone gives us a meaningful way to tune the optical and electronic properties of these molecules.

The enantiomers of **7a**–**c** were separated by HPLC on a semipreparative chiral column. The circular dichroism (CD) and CPL properties of the enantiomers were then studied (Figure 4). Compound **7a** showed a weak Cotton effect at the lowest-energy absorbance (g_{abs} = 1.1 × 10^{-3}; 503 nm), a stronger Cotton effect at the maximum absorbance (g_{abs} = 5.1 × 10^{-3}; 351 nm), and an average g_{lum} of 1.1 × 10^{-3} from 480 to 620 nm. Compound **7b** showed a weak Cotton effect at the lowest-energy absorbance (g_{abs} = 8 × 10^{-4}; 487 nm), a stronger Cotton effect at the maximum absorbance (g_{abs} = 3.6 × 10^{-3}; 344 nm), and an average g_{lum} of 8 × 10^{-4} from 480 to 620 nm. Compound **7c** showed a weak Cotton effect at the lowest-energy absorbance (g_{abs} = 8 × 10^{-4}; 479 nm) and a stronger Cotton effect at the maximum absorbance (g_{abs} = 3.3 × 10^{-3}; 322 nm). Unfortunately, the fluorescence quantum yield of **7c** was too low to obtain CPL data. These values compare favorably to those reported for other highly contorted, chiral organic compounds.[11,13,15,16,22−26]

In summary, we have synthesized novel PAHs through 4-fold alkyne benzannulation onto dibenzoheteroles and fluorenone to explore the effects of incorporating heteroatoms and carbonyls into the backbones of our PAHs as well as the effects of changing the geometries of PAH isomers. We found that there is little difference between the sulfur and oxygen derivatives, though substitution of the heteroatom with a carbonyl results in a large bathochromic shift in the fluorescence of the molecule, albeit with a very short lifetime

Table 2. Photochemical and Electrochemical Properties of Compounds 4a, 4b, and 7a–c

compound	E_{ox1} (V)[a]	E_{red1} (eV)[b]	E_{ox2} (V)[a]	E_{red2} (V)	E_{HOMO} (eV)[d]	E_{LUMO} (eV)[d]	$E_{g(EC)}$ (eV)[e]	λ_{abs} (nm)[f]	$E_{g(opt)}$ (eV)[g]
4a	0.39	–	0.73	–	−5.54	–	–	396	3.13
4b	0.48	–	0.71	–	−5.63	–	–	379	3.28
7a[c]	0.14	−2.47	0.52	–	−5.29	−2.68	2.61	490	2.53
7b[c]	0.23	−2.36	0.61	–	−5.38	−2.79	2.59	489	2.54
7c[c]	0.34	−1.96	0.69	−2.50	−5.49	−3.19	2.30	472	2.63

[a]Half-wave potentials were determined by CV and referenced against the Fc/Fc^+ redox couple. [b]Reduction of **4a** and **4b** was not observed in the electrochemical window. [c]For irreversible processes, the peak value was determined by DPV. [d]Calculated using the equations $E_{LUMO} = -[E(M/M^-) + 5.15\ eV]$ and $E_{HOMO} = -[E(M/M^+) + 5.15\ eV]$, assuming that the energy level of Fc/Fc^+ with respect to the vacuum level is −5.15 eV.[21] [e]Calculated from redox potentials. [f]Absorption wavelengths of the first absorption onset. [g]Estimated from the UV–vis spectra.

https://doi.org/10.1021/acs.orglett.2c04071
Org. Lett. 2023, 25, 226−230

and a very small quantum yield. We also demonstrated that a simple change in geometry can have a drastic impact on the optical and electronic properties of a PAH, shifting the absorbance and fluorescence by roughly 100 and 70 nm, respectively, while increasing the fluorescence quantum yield. The increased degree of steric crowding of a functionalized fjord region relative to a functionalized bay region results in chirality and a twisting of the backbone, reducing the symmetry of the chiral isomer and leading to the observed bathochromic shifts. These results are also supported by electrochemical studies showing the decreases in the HOMO−LUMO gap of the chiral isomers relative to the achiral ones. This provides us with a powerful new tool for tuning the optical and electronic properties of PAHs in the design of molecules for organic electronic applications.

■ ASSOCIATED CONTENT

Data Availability Statement

The data underlying this study are available in the published article and its Supporting Information.

Supporting Information

The Supporting Information is available free of charge at https://pubs.acs.org/doi/10.1021/acs.orglett.2c04071.

Additional experimental details, materials, methods, and NMR spectra (PDF)

■ AUTHOR INFORMATION

Corresponding Author

Wesley A. Chalifoux − *Department of Chemistry, University of Nevada, Reno, Reno, Nevada 89557, United States;* orcid.org/0000-0002-6849-6829; Email: wchalifoux@unr.edu

Authors

Ryan J. Malone − *Department of Chemistry, University of Nevada, Reno, Reno, Nevada 89557, United States*

Jonas Spengler − *Insitut für Organische Chemie, Universität Würzburg, 97074 Würzburg, Germany; Center for Nanosystems Chemistry (CNC), Universität Würzburg, 97074 Würzburg, Germany*

Rachael A. Carmichael − *Department of Chemistry, University of Nevada, Reno, Reno, Nevada 89557, United States*

Khoa Ngo − *Department of Chemistry, University of Nevada, Reno, Reno, Nevada 89557, United States*

Frank Würthner − *Insitut für Organische Chemie, Universität Würzburg, 97074 Würzburg, Germany; Center for Nanosystems Chemistry (CNC), Universität Würzburg, 97074 Würzburg, Germany;* orcid.org/0000-0001-7245-0471

Complete contact information is available at: https://pubs.acs.org/10.1021/acs.orglett.2c04071

Notes

The authors declare no competing financial interest.

■ ACKNOWLEDGMENTS

W.A.C. acknowledges the National Science Foundation (CHE-2102107) for supporting this work. F.W. and J.S. are grateful for financial support from the Deutsche Forschungsgemeinschaft (Grant WU317/23). Funding has been provided by the Alexander von Humboldt Foundation.

■ REFERENCES

(1) Nakahara, K.; Mitsui, C.; Okamoto, T.; Yamagishi, M.; Matsui, H.; Ueno, T.; Tanaka, Y.; Yano, M.; Matsushita, T.; Soeda, J.; et al. Furan fused V-shaped organic semiconducting materials with high emission and high mobility. *Chem. Commun.* **2014**, *50* (40), 5342−5344.

(2) Kukhta, N. A.; da Silva Filho, D. A.; Volyniuk, D.; Grazulevicius, J. V.; Sini, G. Can Fluorenone-Based Compounds Emit in the Blue Region? Impact of the Conjugation Length and the Ground-State Aggregation. *Chem. Mater.* **2017**, *29* (4), 1695−1707.

(3) Wei, Y.; Zheng, A.; Xie, X.; Zhang, J.; He, L.; Wang, P. A Pyrrole-Bridged Bis(oxa[5]helicene)-Based Molecular Semiconductor for Efficient and Durable Perovskite Solar Cells: Microscopic Insights. *ACS Mater. Lett.* **2021**, *3* (7), 947−955.

(4) Reger, D.; Haines, P.; Heinemann, F. W.; Guldi, D. M.; Jux, N. Oxa[7]superhelicene: A π-Extended Helical Chromophore Based on Hexa-*peri*-hexabenzocoronenes. *Angew. Chem., Int. Ed.* **2018**, *57* (20), 5938−5942.

(5) Buchta, M.; Rybáček, J.; Jančařík, A.; Kudale, A. A.; Budéšínský, M.; Chocholoušová, J. V.; Vacek, J.; Bednárová, L.; Císařová, I.; Bodwell, G. J.; et al. Chimerical Pyrene-Based [7]Helicenes as Twisted Polycondensed Aromatics. *Chem. - Eur. J.* **2015**, *21* (24), 8910−8917.

(6) Palata, O.; Andronova, A.; Šámal, M.; Nejedlý, J.; Rybáček, J.; Budéšínský, M.; Bednárová, L.; Pospíšil, L.; Císařová, I.; Starý, I.; et al. Synthesis of (Di)thiahelicenes and Dithiophenohelicenes by [2 + 2+2] Cycloisomerization of Alkynes. *Helv. Chim. Acta* **2022**, *105* (3), e202100225.

(7) Mori, T. Chiroptical Properties of Symmetric Double, Triple, and Multiple Helicenes. *Chem. Rev.* **2021**, *121* (4), 2373−2412.

(8) Deng, Y.; Wang, M.; Zhuang, Y.; Liu, S.; Huang, W.; Zhao, Q. Circularly polarized luminescence from organic micro-/nano-structures. *Light: Sci. Appl.* **2021**, *10* (1), 76.

(9) Greenfield, J. L.; Wade, J.; Brandt, J. R.; Shi, X.; Penfold, T. J.; Fuchter, M. J. Pathways to increase the dissymmetry in the interaction of chiral light and chiral molecules. *Chem. Sci.* **2021**, *12* (25), 8589−8602.

(10) Osswald, P.; Würthner, F. Effects of Bay Substituents on the Racemization Barriers of Perylene Bisimides: Resolution of Atropo-Enantiomers. *J. Am. Chem. Soc.* **2007**, *129* (46), 14319−14326.

(11) Renner, R.; Mahlmeister, B.; Anhalt, O.; Stolte, M.; Würthner, F. Chiral Perylene Bisimide Dyes by Interlocked Arene Substituents in the Bay Area. *Chem. - Eur. J.* **2021**, *27* (46), 11997−12006.

(12) Mahlmeister, B.; Renner, R.; Anhalt, O.; Stolte, M.; Würthner, F. Axially chiral bay-tetraarylated perylene bisimide dyes as non-fullerene acceptors in organic solar cells. *J. Mater. Chem. C* **2022**, *10* (7), 2581−2591.

(13) Yang, W.; Longhi, G.; Abbate, S.; Lucotti, A.; Tommasini, M.; Villani, C.; Catalano, V. J.; Lykhin, A. O.; Varganov, S. A.; Chalifoux, W. A. Chiral Peropyrene: Synthesis, Structure, and Properties. *J. Am. Chem. Soc.* **2017**, *139* (37), 13102−13109.

(14) Yang, W.; Kazemi, R. R.; Karunathilake, N.; Catalano, V. J.; Alpuche-Aviles, M. A.; Chalifoux, W. A. Expanding the scope of peropyrenes and teropyrenes through a facile $InCl_3$-catalyzed multifold alkyne benzannulation. *Org. Chem. Front.* **2018**, *5* (15), 2288−2295.

(15) Bam, R.; Yang, W.; Longhi, G.; Abbate, S.; Lucotti, A.; Tommasini, M.; Franzini, R.; Villani, C.; Catalano, V. J.; Olmstead, M. M.; et al. Four-Fold Alkyne Benzannulation: Synthesis, Properties, and Structure of Pyreno[*a*]pyrene-Based Helicene Hybrids. *Org. Lett.* **2019**, *21* (21), 8652−8656.

(16) Chalifoux, W. A.; Sitaula, P.; Malone, R. J.; Longhi, G.; Abbate, S.; Gualtieri, E.; Lucotti, A.; Tommasini, M.; Franzini, R.; Villani, C.; et al. π-Extended Helical Nanographenes: Synthesis and Photophysical Properties of Naphtho[1,2-*a*]pyrenes. *Eur. J. Org. Chem.* **2022**, *2022* (17), e202101466.

(17) Yang, W.; Monteiro, J. H. S. K.; de Bettencourt-Dias, A.; Catalano, V. J.; Chalifoux, W. A. Pyrenes, Peropyrenes, and Teropyrenes: Synthesis, Structures, and Photophysical Properties. *Angew. Chem., Int. Ed.* **2016**, *55* (35), 10427−10430.
(18) Yang, W.; Monteiro, J. H. S. K.; de Bettencourt-Dias, A.; Catalano, V. J.; Chalifoux, W. A. Synthesis, Structure, Photophysical Properties, and Photostability of Benzodipyrenes. *Chem. - Eur. J.* **2019**, *25* (6), 1441−1445.
(19) Yang, W.; Bam, R.; Catalano, V. J.; Chalifoux, W. A. Highly Regioselective Domino Benzannulation Reaction of Buta-1,3-diynes To Construct Irregular Nanographenes. *Angew. Chem., Int. Ed.* **2018**, *57* (45), 14773−14777.
(20) Rieger, R.; Müllen, K. Forever young: polycyclic aromatic hydrocarbons as model cases for structural and optical studies. *J. Phys. Org. Chem.* **2010**, *23* (4), 315−325.
(21) Cardona, C. M.; Li, W.; Kaifer, A. E.; Stockdale, D.; Bazan, G. C. Electrochemical Considerations for Determining Absolute Frontier Orbital Energy Levels of Conjugated Polymers for Solar Cell Applications. *Adv. Mater.* **2011**, *23* (20), 2367−2371.
(22) Würthner, F. Bay-substituted perylene bisimides: Twisted fluorophores for supramolecular chemistry. *Pure Appl. Chem.* **2006**, *78* (12), 2341−2349.
(23) Reine, P.; Ortuño, A. M.; Mariz, I. F. A.; Ribagorda, M.; Cuerva, J. M.; Campaña, A. G.; Maçôas, E.; Miguel, D. Simple Perylene Diimide Cyclohexane Derivative With Combined CPL and TPA Properties. *Front. Chem.* **2020**, *8*, 306.
(24) Liu, B.; Böckmann, M.; Jiang, W.; Doltsinis, N. L.; Wang, Z. Perylene Diimide-Embedded Double [8]Helicenes. *J. Am. Chem. Soc.* **2020**, *142* (15), 7092−7099.
(25) Wade, J.; Brandt, J. R.; Reger, D.; Zinna, F.; Amsharov, K. Y.; Jux, N.; Andrews, D. L.; Fuchter, M. J. 500-Fold Amplification of Small Molecule Circularly Polarised Luminescence through Circularly Polarised FRET. *Angew. Chem., Int. Ed.* **2021**, *60* (1), 222−227.
(26) Zhang, L.; Song, I.; Ahn, J.; Han, M.; Linares, M.; Surin, M.; Zhang, H.-J.; Oh, J. H.; Lin, J. π-Extended perylene diimide double-heterhelicenes as ambipolar organic semiconductors for broadband circularly polarized light detection. *Nat. Commun.* **2021**, *12* (1), 142.

https://doi.org/10.1021/acs.orglett.2c04071
Org. Lett. 2023, 25, 226−230